Anomalous evolution of aerodynamic roughness and shear velocity on large flows

M.Y. Louge, *Mechanical Engineering, Cornell University, Ithaca, NY, USA – MYL3@cornell.edu*
A. Valance, *Institut de Physique de Rennes, Université de Rennes, Rennes, France*
J. Fang, *Ecole Polytechnique Fédérale de Lausanne, Lausanne, Switzerland*
S. Harnett, *Mechanical Engineering, Cornell University, Ithaca, NY, USA*
F. Porté-Angel, *Ecole Polytechnique Fédérale de Lausanne, Lausanne, Switzerland*
P. Chasle, *Institut de Physique de Rennes, Université de Rennes, Rennes, France*

ABSTRACT: We recorded aerodynamic roughness and shear velocity along transects on and around crescent-shaped barchan dunes of 4.5 m and 27 m height in the Qatar desert. The data revealed unexpected evolution of aerodynamic roughness from very large on the desert floor to much lower than the prescription of Nikuradse (1933) for a smooth surface. While qualitatively conforming to the predictions of Jackson and Hunt (1975), the shear velocity also exhibited an anomalously high value at the slope discontinuity between the upwind and avalanche faces. These measurements call into question the formulation of boundary conditions in numerical simulations over evolving bedforms, whether they are designed for aeolian or marine experiments.

1 INTRODUCTION

Turbulent flows over large bedforms are difficult to compute with fidelity (Smyth 2016). Most efforts have focused on improving the size and resolution of numerical simulations, by scaling-up the domain of methods such as Large-Eddy-Simulations (LES) (Stoll & Porté-Agel 2006, Omidyeganeh & Piomelli 2013, Fang & Porté-Agel 2016, Liu et al. 2019, Hardy et al. 2021, Zheng et al. 2021, Jin et al. 2021), Reynolds-Averaged Navier-Stokes (RANS) (Jin et al. 2021, Lane et al. 2004, Lefebvre et al. 2014, Michelsen et al. 2015), or methods coupling morphodynamics with a fluid mechanics solver such as Lattice methods (Narteau et al. 2019, Lü et al. 2018, Zhang et al. 2022), LES or RANS (Sotiropoulos & Khosronejad 2016).

However, less attention has been paid to verifying boundary conditions at the surface on the geophysical scale. As suggested by Launder and Spalding (1974), most models adopt a condition that relates shear stress $\tau_0 = \rho\, u^{*2}$ on the surface to velocity in the next grid cell aloft, as prescribed by the profile in the core of the turbulent boundary layer,

$$u(z) = \frac{u^*}{\kappa} \ln\left(\frac{z}{z_0}\right) \quad (1)$$

where u* is the shear velocity, z is elevation above the surface, ρ is the fluid density, κ=0.41 is von Kármán's constant, and z_0 is an effective aerodynamic roughness. In fluvial environments, the Chézy condition (Lefebvre et al. 2004, D'Ippolito et al. 2021) amounts to a similar prescription. If the domain is small enough that the solver can resolve the viscous sublayer explicitly, for example on sand ripples (Jin et al. 2022) or in laboratory-scale bedforms in flumes (Omidyeganeh & Piomelli 2013), then a no-slip condition u = 0 may instead be imposed at z = 0. However, the required space discretization is, for the capabilities of current machines, too fine to handle large objects such as desert or submarine dunes.

Meanwhile, Eq. 1 alone does not account for the role of the inertial inner layer that Jackson and Hunt (1975) discovered. These authors showed that, over a low hill, gas

inertia compels the maximum shear stress to arise upstream of the maximum speed at the hill crest. Unfortunately, because numerical simulations rarely resolve the thickness of this inner layer, they cannot capture this important effect, which contributes to dune inception (Kroy et al. 2002).

Another common situation is to find dunes surrounded by a flat desert floor covered with stones. For instance, in our field of barchans, sands of 351 μm mean diameter were surrounded by rocks of decimetric size (Louge et al. 2013), thereby creating a sharp discontinuity in geometrical surface roughness. While it is possible to simulate a complicated rugged bedform topography on the size of flume experiments (Hardy et al. 2021), such endeavor is not feasible in the field. Instead, to handle geophysical scales in such meteorological situations as wind transitioning from the ocean to a coastal forest, Walmsley et al (1986) incorporated an evolution of geometrical roughness within the framework of Jackson and Hunt (1975).

In general, one implicitly assumes that aerodynamic roughness z_0 is related to its geometrical counterpart. For turbulent flows in *smooth* pipes, reconciling Eq. 1 with the universal turbulent core profile in wall units yields an effective aerodynamic 'roughness' satisfying

$$\ln\left(\frac{u^* z_0}{\nu}\right) = -a_u \kappa \quad (2)$$

where a_u=5.1 and ν is the kinematic fluid viscosity. However, as u* rises with pipe Reynolds number, Nikuradse (1933) showed that the Darcy friction factor reaches an asymptote that becomes invariant with u*, but that now depends on the geometrical size of wall roughness. By integrating the velocity profile in Eq. 1 for internal turbulent flows in pipes, one can recover the measured Darcy friction coefficient and, reconciling it with the asymptotic data of Nikuradse (1933) for internal pipe wall roughened with sand of diameter d, extract the classical effective aerodynamic roughness at high u*,

$$z_0 \simeq \frac{d}{\omega} \quad (3)$$

where ω≃33. This expression, which captures the limit of large roughness or large Reynolds number, now explicitly involves a geometrical characterization of surface bumps. Assuming a universal character of wall-bound turbulence, it is commonly adopted even for external flows that do not resemble Nikuradse's pipes, for example on the surface of sand dunes at sufficiently large u∗ (Andreotti et al. 2002). However, as the next section shows, we found instances where aerodynamic roughness is considerably smaller than what Eqs. 2 or 3 suggest.

2 FIELD EXPERIMENTS

We measured shear velocity and aerodynamic roughness by positioning triads of ultrasonic anemometers to penetrate the inertial inner layer described by Jackson and Hunt (1975). All measured profiles closely conformed to the log-law for the core of turbulent boundary layers. As Fig. 1 illustrates, shear velocity first decreased, then recovered as air climbed on the small dune along a centerline transect, with a local maximum ahead of the crest as Jackson and Hunt (1975) predicted.

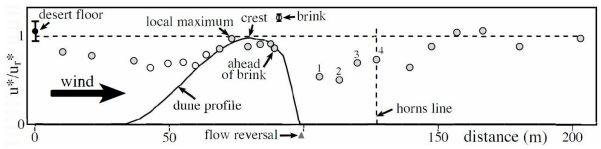

Figure 1: Shear velocity relative u* to its value at the crest u_r* along the transect on the centerline of a barchan dune of 4.5 m height.

At odds with existing models of the downstream dune wake (Kroy et al. 2002), an anomalous peak of shear velocity arose on the dune centerline at the brink. By forsaking descriptions of the wake as a bubble bound by a solidified streamline (Kroy et al. 2002), our direct application of the theory of Jackson and Hunt (1975) to the actual dune shape, including its discontinuous slope at the brink, suggested the origin of such anomaly (Louge et al. 2023).

We also recorded the evolution of aerodynamic roughness along the same transect, from its high value on the rough desert floor to lower ones on the dune and its wake. To question whether the Nikuradse (1993) formulation remained valid, we referred aerodynamic roughness to its asymptotic geometrically-rough limit in Eq. 3 and defined $\ln z_0\dagger = \ln(z_0\,\omega/d)$. If, as is often expected, $\ln z_0$ cannot fall below its asymptotic value $\ln(d/\omega)$ at large shear velocity, then one should always observe $\ln z_0\dagger>0$. However, as Fig. 2 shows, there are locations near the dune's upstream toe where this inequality is not met.

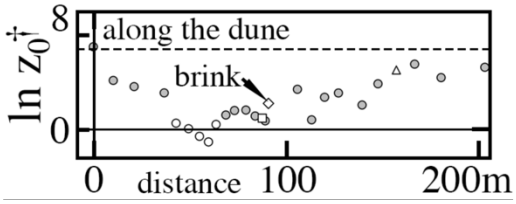

Figure 2: Log of the aerodynamic roughness relative to its value at high u*, $\ln z_0\dagger= \ln(z_0\,\omega/d)$, vs distance along the transect of Fig. 1.

Figure 3 confirms these observations along a similar transect on the larger dune of 27 m height. There, we also observed a peak of shear velocity at the brink, as well as sharply negative $\ln z_0\dagger$. More remarkably, values of $\ln z_0$ recorded near the upwind toe were even smaller than those prescribed by Eq. 2 for a smooth surface (dotted line).

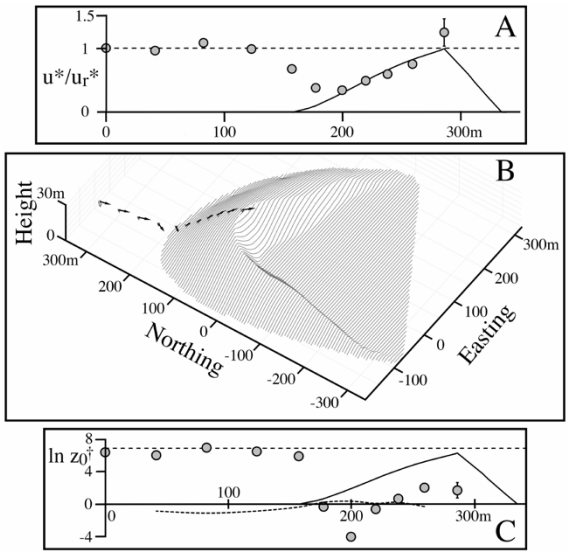

Figure 3: Observations on the larger dune of 27.2 m height. (A) Profile of u^*/u_r^* along the transect shown in (B). The horizontal dashed line marks $u^*=u_r^*$, where u_r^* is the reference shear velocity that we simultaneously recorded with a fixed anemometer triad upstream of the dune, on the origin of distances plotted. (B) Dune topography with superimposed roving anemometer positions and arrows proportional to u^*/u_r^* and aligned with the wind velocity. (C) Profile of $\ln z_0\dagger$ along the transect. The dashed horizontal straight line is $\ln z_0\dagger=6.9$ from Louge, et al. (2023). The dotted line is aerodynamic roughness for a smooth surface (Eq. 2). In (A) and (C), the solid line shows dune altitude along the transect with an arbitrary scale.

3 CONCLUSIONS

Turbulent boundary conditions on the surface of large isolated barchan dunes standing on a rough, nearly horizontal desert floor are not as straightforward to specify as what numerical simulations typically prescribe. First, we found that it is important to resolve the relatively thin inner layer described by Jackson and Hunt (1975). Without such precaution, a simulation is unlikely to capture the peaking of surface shear stress ahead of the dune crest, or the existence of a sharp maximum of shear velocity at the brink, both of which are associated with the inner layer.

Second, we observed that, as the log of aerodynamic roughness evolves from a relatively large value on the stone-covered desert floor to the smoother dune, this quantity can descend well below the classical model derived from data for internal flows in rough pipes (Nikuradse 1933). Therefore, sadly, it appears that numerical simulations of large, field-size bedforms must resolve the turbulent boundary layer closely, at least through the inner layer – and possibly closer to the surface –, so the evolution of aerodynamic roughness can be properly captured.

These observations should also be relevant to marine and fluvial bedforms, which are subject to similar variations in detailed topography between sea floor and dunes, and which also possess slope discontinuities where gravity currents first arise.

In this context, dune fields with steady, nearly unidirectional winds constitute a natural laboratory where turbulent surface boundary conditions may be measured at scale.

We are currently writing an article (Louge et al. 2023) that presents our desert data in greater detail, including their interpretation within the Jackson and Hunt framework (Jackson & Hunt 1975, Kroy et al. 2002), the existence of multiple thresholds of sand entrainment, and variations of shear velocity and aerodynamic roughness during aeolian transport through the lens of Bagnold's focal point in the turbulent boundary layer (Bagnold 1941, Jenkins & Valance 2014).

4 ACKNOWLEDGMENT

This work was made possible by the support of NPRP grants 09-546-2-206 and 6-059-2-023 from the Qatar National Research Fund, and a Qatar Foundation Research Excellence Award. This research was supported in part by the National Science Foundation under Grant No. NSF PHY-1748958.

5 REFERENCES

Andreotti, B., Claudin, P., and Douady, S. (2002). Selection of dune shapes and velocities. Part 1: Dynamics of sand, wind and barchans. The European Physical Journal B-Condensed Matter and Complex Systems 28, 321-339. doi:10.1140/epjb/e2002-00236-4.

Bagnold, R. A. (1941). The physics of blown sand and desert dunes. Chapman and Hall, Methuen, London.

D'Ippolito, A., Calomino, F., Alfonsi, G. and Lauria, A. (2021). Flow resistance in open channel due to vegetation at reach scale: a review. Water 13, 116:1-27. doi:10.3390/w13020116.

Fang, J. and Porté-Agel, F. (2016). Intercomparison of terrain-following coordinate transformation and immersed boundary methods in large-eddy simulation of wind fields over complex terrain. J. Phys. Conf. Ser. 753:082008. doi:10.1088/1742-6596/753/8/082008.

Hardy, R. J., Best, J. L., Marjoribanks, T. I., Parsons, D. R., and Ashworth, P. J. (2021). The influence of three-dimensional topography on turbulent flow structures over dunes in unidirectional flows. Journal of Geophysical Research: Earth Surface 126, e2021JF006121. doi:10.1029/2021JF006121.

Jackson, P. S. and Hunt, J. C. R. (1975). Turbulent wind flow over a low hill. Quart. J. R. Met. Soc. 101:929–955. doi:10.1002/qj.49710143015.

Jenkins, J.T., and Valance, A (2014): Periodic trajectories in aeolian sand transport. Physics of Fluids 26, 073301. doi:10.1063/1.4885576.

Jin, T., Wang, P., and Zheng, X. (2021). Characterization of wind-blown sand with near-wall motions and turbulence: From Grain-scale distributions to sediment transport. Journal of Geophysical Research: Earth Surface 126, e2021JF006234. doi:10.1029/2021JF006234.

Jin, C., Coco, G., Tinoco, R. O., Ranjan, P., Gong, Z., Dutta, S., San Juan, J. E., and Friedrich, H. (2022). High resolution Large Eddy Simulations of vortex dynamics over ripple defects under oscillatory flow. Journal of Geophysical Research: Earth Surface 127, e2021JF006328. doi:10.1029/2021JF006328.

Kroy, K., Sauermann, G. and Herrmann, H. J. (2002). Minimal model for sand dunes. Phys. Rev. Lett. 88:054301, doi:10.1103/PhysRevLett.88.054301.

Lane, S. N., R. J. Hardy, L. Elliott, and D. B. Ingham (2004). Numerical modeling of flow processes over gravelly surfaces using structured grids and a numerical porosity treatment. Water Resources Research 40, W01302. doi:10.1029/2002WR001934.

Launder, B.E., and Spalding, D.B. (1974). The numerical computation of turbulent flows. Computer Methods in Applied Mechanics and Engineering 3, 269-289. doi:10.1016/0045-7825(74)90029-2.

Lefebvre, A., A. J. Paarlberg, and C. Winter (2014). Flow separation and shear stress over angle-of-repose bed forms: A numerical investigation. Water Resources Research 50, 986-1005. doi:10.1002/2013WR014587.

Liu, Y., Fang, H., Huang, L. and He, G. (2019). Numerical simulation of the production of three-dimensional sediment dunes. Physics of Fluids 31, 096603. doi:10.1063/1.5108741.

Louge, M.Y., Valance, A., Ould el-Moctar, A., Xu, J., Hay, A.G., and Richer, R. (2013). Temperature and humidity within a mobile barchan sand dune, implications for microbial survival. J. Geophys. Res. Earth Surf. 118, 1-14. doi:10.1002/2013JF002839.

Louge, M.Y., Valance, A., Fang, J., Harnett, S., Porté-Agel, F., and Chasle, P. (2023). Evolution of turbulent boundary conditions on the surface of large barchan dunes: anomalies in aerodynamic roughness and shear velocity, aeolian thresholds and the role of dune skewness. J. Geophys. Res. Earth Surf., in preparation.

Lü, P., Dong, Z., and Rozier, O. (2018). The combined effect of sediment availability and wind regime on the morphology of aeolian sand dunes. Journal of Geophysical Research: Earth Surface 123, 1-9. doi:10.1029/2017JF004361.

Michelsen, B., Strobl, S., Parteli, E.J. and Pöschel, T (2015). Two-dimensional airflow modeling underpredicts the wind velocity over dunes. Scientific reports 5, 1-8. doi:10.1038/srep16572.

Narteau, C., Zhang, D., Rozier, O., and Claudin, P. (2009). Setting the length and time scales of a cellular automaton dune model from the analysis of superimposed bed forms. Journal of Geophysical

Research: Earth Surface 114, 1-18. doi:10.1029/2008JF001127.

Nikuradse J. (1933). Strömungsgesetze in rauhen Rohren (Laws of Flow in Rough Pipes). Forschung auf dem Gebiete des Ingenieurwesens, Ausgabe B Band 4:1-62, NACA Technical Memorandum 1292, Washington, D.C.

Omidyeganeh, M. and Piomelli, U. (2013). Large-eddy simulation of three-dimensional dunes in a steady, unidirectional flow. Part 1. Turbulence statistics. Journal of Fluid Mechanics 721, 454-483. doi:10.1017/jfm.2013

Sotiropoulos, F. and Khosronejad, A. (2016). Sand waves in environmental flows: Insights gained by coupling large-eddy simulation with morphodynamics. Physics of Fluids 28, 021301. doi:10.1063/1.4939987.

Smyth, T.A. (2016). A review of Computational Fluid Dynamics (CFD) airflow modelling over aeolian landforms. Aeolian research 22:153-164. doi:10.1016/j.aeolia.2016.07.003.

Stoll, R. and Porté-Agel, F. (2006). Dynamic subgrid-scale models for momentum and scalar fluxes in large-eddy simulations of neutrally stratified atmospheric boundary layers over heterogeneous terrain. Water Resources Research 42, W01409:1-18. doi:10.1029/2005WR003989.

Walmsley, J.L., Taylor, P.A. and Keith, T. (1986). A simple model of neutrally stratified boundary-layer flow over complex terrain with surface roughness modulations (MS3DJH/3R). Boundary-Layer Meteorology 36, 157-186. doi:10.1007/BF00117466.

Zhang, Q., Deal, E., Perron, J. T., Venditti, J. G., Benavides, S. J., Rushlow, M., and Kamrin, K. (2022). Fluid-driven transport of round sediment particles. From discrete simulations to continuum modeling. Journal of Geophysical Research: Earth Surface 127, e2021JF006504. doi:10.1029/2021JF006504.

Zheng, X., Jin, T., and Wang P. (2020). The influence of surface stress fluctuation on saltation sand transport around threshold. Journal of Geophysical Research: Earth Surface 125, e2019JF005246. doi:10.1029/2019JF005246.